Journal of Magnetic Resonance **146,** 321–334 (2000)
doi:10.1006/jmre.2000.2150, available online at http://www.idealibrary.com on IDEAL®

Stable Reconstruction of the T_2 Distribution by Low-Resolution NMR Measurements and the Classical Markov and Hausdorf Momentum Problem

Gy. Steinbrecher,* R. Scorei,† V. M. Cimpoiasu,† and I. Petrisor‡

*Association EURATOM, International Working Group "Fusion B.F.R.," Department of Theoretical Physics, †Department of Biochemistry, and ‡Department of Experimental Physics, University of Craiova, 1100 Craiova, Dolj, Romania

Received February 7, 2000; revised June 19, 2000

Assuming that an original distribution is a probabilistic measure and the Laplace transforms are known only for a finite number of points that are affected by errors, we develop a method for reconstructing weak-sense mean values obtained by integrating smooth functions with the measure. Our method is useful in NMR if the NMR signal can be represented as a superposition of exponential terms. In these circumstances, we show how the data processing can be related to the classical Hausdorf momentum problem. First, we clarify the meaning of stable spectrum reconstruction, and then develop stable filtering and a mean value reconstruction algorithm. Our method has been tested on both simulated and real sets of spin–spin relaxation curves with noise. In view of this, our method could provide an efficient and accurate reconstruction of spin–spin relaxation data. For any reader interested in applications, a "practical recipe" that is almost self-consistent has been included.

Key Words: **time domain; NMR; relaxation; classical momentum problem; numerical Laplace transform inversion.**

I. INTRODUCTION

In the interpretation of the spin–spin relaxation data, the first temptation is to invert the Laplace transform, in order to recover population densities and relaxation times. An almost similar mathematical problem was treated extensively in (*1*), where the difficulties related to the numerical inversion of the Laplace transform are solved in the special case of a known upper bound on the number of populations (exponential terms). In most situations, the restrictions imposed in (*1*) are not satisfied (there is no upper bound on the number of populations, and, moreover, there can be an infinity of them). In this work, we solve such a generalized reconstruction problem. The final recipe is given in Section VII.

In most previous works the computation of NMR parameters, such as relaxation times and populations, is strongly dependent on the particular details of the reconstruction algorithm; in other words, the reconstruction is unstable.

In this paper we suppose that the dependence on time of the NMR ideal noiseless signal $s(t)$ for T (spin–spin relaxation time) may be represented as (*2*)

$$s(t) = \sum_{i=1}^{N} n_i \exp(-t/T_i),\ n_i \geq 0,\ \sum_{i=1}^{N} n_i = 1,\ T_i > 0, \quad [1a]$$

where n_i and T_i are the populations and the relaxation times, respectively.

Due to lack of information on n_i and T_i, we are forced to consider the more general representation

$$s(t) = \int_{T_{\min}}^{T_{\max}} \exp(-t/\tau)\, d\rho(\tau) = \sum_{i=1}^{N} n_i \exp(-t/T_i) + \int_{T_{\min}}^{T_{\max}} \exp(-t/\tau)\varphi(\tau)\, d\tau. \quad [1b]$$

In Eq. [1b] $\rho(\tau)$ is a Borel measurable nondecreasing function whose continuous part of $\varphi(\tau)$ is associated with a continuous relaxation time spectrum, typical in nonhomogeneous disperse or multiphase media, and the jump points of $\rho(\tau)$, (T_i), correspond to the discrete spectrum. We denote by $T_{\min}$ and $T_{\max}$ the known bounds on relaxation times, obtained from other experiments or theoretical models. The simplest, but naïve, question that one may raise is how to compute the populations n_i and the relaxation times T_i, or, more generally, the distribution function $\rho(\tau)$ from the sequence of samples affected by errors ($s'_k = s(k\Delta t) + \Delta s_k$, where Δs_k is the experimental error). As explained in Section III, the direct reconstruction of the populations n_i and the relaxation times T_i is impossible if N from Eq. [1a] is not known, because of the mathematical instability of the problem itself, even in the idealized noiseless case, when $s(t)$ is known in a finite number of points. Nevertheless, as we show in Section II, we could compute some mean values, of the form $\int_{T_{\min}}^{T_{\max}} f(\tau)\, d\rho(\tau)$, for some especially

1090-7807/00 $35.00

selected $f(\tau)$, directly from $s(t)$, without computing n_i, T_i, or $d\rho(\tau)$, shortcutting the reconstruction instability of the measure $d\rho(\tau)$ (or n_i and T_i).

In Section II we expose a simple and stable method that could be applied directly to extract some global information on n_i and T_i, without sharp localization of T_i. This result is the starting point, which justifies a more rigorous treatment.

In Section III we expose the connection to the classical momentum problem (*3, 4*) and describe the filtering algorithm of the noise-perturbed data.

In Section IV we generalize and clarify the results from Sections II and III by solving the reconstruction problem from noisy s'_k for the mean values $\int_{T_{\min}}^{T_{\max}} f(\tau)d\rho(\tau)$, if $f(\tau)$ is a smooth and at least continuously differentiable on the $T_{\min} \le \tau \le T_{\max}$ function.

In Sections V and VI we apply the mathematical method from Section IV to a series of simulated and experimental signals.

In the followings we consider $T_{\min}$ or $T_{\max}$ to be known, $0 \le T_{\min} < T_{\max} \le \infty$. In case we have no extra information (which could increase effectiveness), even in the extreme cases of lack of information ($T_{\min} = 0$ and/or $T_{\max} = \infty$), our results are still valid.

Without any loss of generality, we can consider $s(\tau)$ normalized as $s(0) = 1$, or $\int_{T_{\min}}^{T_{\max}} d\rho(\tau) = 1$; i.e., $d\rho$ is a probabilistic measure, respectively, $\sum_{i=1}^{N} n_i = 1$, for discrete distribution and n_i can be interpreted in probabilistic framework.

The case where N from Eq. [1a] is known can be found in (*1*), so this can be considered a solved problem, at least when N is not too large.

Thus, the essential point is the following (perhaps a little deceptive) statement: the reconstruction of T_i and n_i from Eq. [1a] or $\rho(\tau)$ ($\varphi(t)$) from Eq. [1b] is impossible, but we can reconstruct a "smeared out" or "convoluted" distribution, which could give some "fuzzy" information on the relaxation times and populations. The basic argument for the impossibility of direct reconstruction is the intrinsic mathematical instability, a consequence of the nonuniqueness of the finite-input classical momentum problem. This does not mean that the reconstruction in TD low-resolution NMR should be abandoned. Though at different scales, we can compare this situation with the impossibility of long-term prediction in unstable chaotic deterministic systems (fluid dynamics, meteorology, and celestial mechanics) or classical statistical physics and molecular dynamics where, although the trajectories of molecules depend sensitively on initial conditions, the macroscopic observables can be computed in a safe manner, as mean values of microscopic quantities.

II. DIRECT RECONSTRUCTION OF MEAN VALUES (WITHOUT NONLINEAR FILTERING)

All of these calculations can be performed easily on a small programmable pocket calculator in an extremely stable manner. For readers interested in applications using a powerful PC, this part may be skipped.

Despite the fact that filtering increases efficiency, there is a simple quick algorithm (without filtering) for some mean value computations, which can be implemented in stable form: the mean values $\langle T^\alpha \rangle$ can be computed from the identity

$$\langle T^\alpha \rangle \overset{\text{Def}}{=} \int_{T_{\min}}^{T_{\max}} T^\alpha d\rho(T) = \frac{1}{\Gamma(\alpha)} \int_0^\infty t^{\alpha-1} s(t) dt, \qquad [2]$$

or $\langle T^\alpha \rangle = \sum_{i=1}^{N} T_i^\alpha n_i$, for discrete distributions. For simplicity, we prove Eq. [2] in the case: using Eq. [1a], we obtain

$$\int_0^\infty s(t) t^{\alpha-1} dt = \int_0^\infty \sum_{i=1}^{N} \exp(-t/T_i) t^{\alpha-1} n_i dt$$

$$= \sum_{i=1}^{N} n_i \int_0^\infty \exp(-t/T_i) t^{\alpha-1} dt.$$

The integrals can be reduced to the Euler gamma function $\Gamma(\alpha) = \int_0^\infty \exp(-y) y^{\alpha-1} dy$ by substitution $y = t/T_i$. α is a complex number, with $\mathrm{Re}(\alpha) > 0$, but not too large. Then Eq. [2] follows immediately from Eq. [1b] and the definition of $\langle T^\alpha \rangle$.

Let us suppose that: (a) we have a good numerical interpolation of $s(k\Delta t) \approx s(t)$ necessary for numerical integration; and (b) there is an upper cutoff Λ, such that we could approximate the integrals

$$\int_0^\infty s(t)(\ldots) dt \approx \int_0^\Lambda s(t)(\ldots) dt \qquad [3]$$

(Λ is less or equal to the measuring time).

In Eq. [2] we have two kinds of numerical instabilities: If $\mathrm{Re}(\alpha) < 1$, the instabilities that appear at $t \approx 0$ and, if α is large, the incertitude in Eq. [3] at large t.

A good choice appears to be $\alpha = 1$, when we obtain

$$\langle T \rangle = \int_0^\infty s(t) dt \cong \int_0^\Lambda s(t) dt$$

(the arithmetic mean value of relaxation time),

which was used in (*5, 6*).

Because $\Gamma(n) = (n-1)!(n \in Z_+)$, we can compute

$$\langle T^2 \rangle = \int_0^\infty t \cdot s(t) dt, \; \langle T^3 \rangle = \frac{1}{2} \int_0^\infty t^2 s(t) dt,$$

$$\langle T^4 \rangle = \frac{1}{3!} \int_0^\infty t^3 s(t) dt,$$

which gives

$$\sigma^2 = (\langle T^2\rangle - \langle T\rangle^2) \text{ (the dispersion)},$$
$$a_s = \frac{\langle T - \langle T\rangle\rangle^3}{\sigma^3} \text{ (the asymmetry)},$$
$$k = \frac{\langle T - \langle T\rangle\rangle^4}{3\sigma^4} \text{ (the kurtosis)}.$$

We can compute also the displaced by T_0 "harmonic mean value," T_h,

$$\left\langle \frac{1}{\tau + T_0} \right\rangle \overset{\text{Def}}{=} \int_{T_{\min}}^{T_{\max}} \frac{d\sigma(\tau)}{\tau + T_0} \overset{\text{Def}}{=} \frac{1}{T_h + T_0},$$

using Eq. [A1] and its dispersion (see Appendix A).

The drawback of these methods is the following: (a) computation of higher moments $\langle T^2\rangle$, $\langle T^3\rangle$, and $\langle T^4\rangle$ can be strongly affected by errors of $s(t)$ for large t; (b) the harmonic mean values are insensitive on the large T components of $d\sigma(\tau)$; (c) even in small error cases, we do not obtain localized information.

III. CONNECTION TO THE CLASSICAL MOMENTUM PROBLEM AND NONLINEAR FILTERING OF DATA

III.1. Existence of Representation [1b] and Necessity of Filtering

The noiseless part of the signal sequence

$$s_k = s(k\cdot\Delta t) = \int_{T_{\min}}^{T_{\max}} \exp(-k\Delta t/\tau)\, d\rho(\tau),$$
$$d\rho(\tau) \geq 0,\ k = \overline{0,\ M}, \qquad [4a]$$

by substitution $x = \exp(-k\Delta t/\tau)$, $\sigma(e^{-\Delta t/\tau}) = \rho(\tau)$, can be rewritten as

$$s_k = \int_a^b x^k d\sigma(x),\ k = \overline{0,\ M},\ d\sigma(x) \geq 0, \qquad [4b]$$

where

$$a = \exp(-\Delta t/T_{\min}),\ b = \exp(-\Delta t/T_{\max}),\ 0 \leq a < b \leq 1. \qquad [4c]$$

The unphysical variable x will be important in the following, relating our NMR problem to a standard mathematical one. The study of the properties of $d\sigma(x)$, starting from Eq. [4b] is a classical, but still actual problem of functional analysis (*3, 4, 7*). For $M = 2$, this problem has a clean mechanical interpretation. Let an inhomogeneous rod, with constant cross section placed on $0x$ axis, be between a and b, and let $\sigma(x)$ the (unknown) total mass be between a and x. Then s_0, s_1, s_2 are the total mass, baricenter, and inertia moment. Then our problem is to find as much as information about mass distribution $\sigma(x)$, knowing only s_0, s_1, s_2. When $M = \infty$, Eq. [4] is known as the Hausdorf momentum problem, while for M finite this is the Markov or incomplete Hausdorf momentum problem. The incomplete Hausdorf momentum problem is related to the problem of extrapolation for analytic functions (*7*). The general aspects of stability questions in numerical computations, with applications to the scattering theory of elementary particles, were treated in (*8, 9*). An adaptation of a generalized Markov momentum problem to lattice gauge theory computation was proposed in (*10*) and in the quantum few-body problem, in (*11*).

Contrary to intuition, the conditions $n_i \geq 0$ from Eq. [1a] or $d\sigma(x) \geq 0$ from Eq. [4b] give rise to very strong restrictions when M is large, given by the following Proposition 1 (*7*). For reader's convenience we anticipate that these conditions in experimental situations are never fulfilled. Nevertheless, this issue is conceptually influencing the present work.

PROPOSITION 1. The restrictions on s_k. The representation [4] of s_k as moments of a positive measure stands if and only if the following quadratic forms Q_1 and Q_2 are nonnegative (we will abbreviate these restrictions by (**R**)).

(a) M: even. We define $s_k^{(1)} = -s_{k+2} + (a+b)s_{k+1} - ab\, s_k$, $k = \overline{0,\ M-2}$, then $Q_1 = \sum_{m,n=0}^{M-2} s_{m+n}^{(1)} \bar{z}_m z_n$ and $Q_2 = \sum_{m,n=0}^{M} s_{m+n} \bar{z}_m z_n$.

(b) M: odd. $s_k^{(2)} = b\cdot s_k - s_{k+1}$, $k = \overline{0, M-1}$. $s_k^{(3)} = s_{k+1} - a\cdot s_k$, $k = \overline{0, M-1}$, then $Q_1 = \sum_{m,n=0}^{M-1} s_{m+n}^{(2)} \bar{z}_m z_n$, $Q_2 = \sum_{m,n=0}^{M-1} s_{m+n}^{(3)} \bar{z}_m z_n$.

We emphasize that the necessity of these conditions for Eq. [1b] is elementary to check. Sufficiency is more difficult. In the NMR terminology, for the noiseless, ideal signal samples, representation $s(k\Delta t) = \sum_{i=1}^{N} n_i \exp(-k\Delta t/T_i)$ (or more generally Eq. [4a]) is possible, with $n_i \geq 0$, $T_{\min} < T_i \leq T_{\max}$ if and only if the restrictions (**R**) are fulfilled, with a and b given by Eq. [4c]. If (**R**) are fulfilled, we could use the whole collection of analytical methods (*7*). We denote by K_M the set of all vectors $\{s_k\}_1^M \in R^M$, which satisfies (**R**) and $s_0 = 1$, i.e., the set of all ideal normalized signal samples. Clearly K_M is a closed bounded convex subset of R^M. For convexity remarks, see below.

At first sight we can expect that if experimental error would be small, the above conditions should be fulfilled and we could use the whole classical theory and use (**R**) to reject some data. The numerical tests and analytical results (explained in Appendix B) show the probability that the error-affected signal $s'_k = s(k\Delta t) + \Delta s_k$ fulfills (**R**) is very small, and if $M \geq 5$ it should be meaningless to test. If we use (**R**) to reject some data, all of them will be rejected.

This is a very important fact, mainly for readers who will be

tempted to learn unnecssary topics on classical momentum problem, for further developments. In order to prove the above statement, we use in Appendix B the elegant result of Karlin and Shapley (*17*). Translated in NMR terminology, they in fact hopefully computed the probability that a sequence of signal samples $0 \leq s_k \leq 1$ taken randomly and independently, all uniformly distributed on [0, 1], could be written as Eq. [1a] or Eq. [1b], i.e., to be an ideal, noiseless true physical NMR signal (for details see Appendix B), although in theirs paper (*17*) there is no reference to NMR and probabilities.

Therefore, if $M \geq 5$, the test of positivity conditions is meaningless because it is too restrictive and practically never fulfilled. In order to work in a mathematically correct context, we must replace the experiment sequence s'_k by another sequence, which (a) satisfies (**R**), and (b) approximates s'_k optimally. The convexity of the set K_M is an important fact. Similar to, e.g., 2- and 3-dimensional cases, the closest point from K_M to a point outside of this set is always on the boundary. But because the interior points in Eq. [1b] are those with $n_i > 0$, the boundary points will be of $n_i = 0$ (in fact, in many of the practical applications, only few (<10) are nonzero).

III.2. The Filtering

Next we cope with the following problem: Find the best approximation of the perturbed-by-noise data s'_k by some $\{s_k\} \in K_M$, i.e., by some ideal, normalized signal sequence. If the noise is not correlated, stationary, and additive, then the rigorous meaning would be to find the sequence $\{s_k\} \in K_M$ that realizes the optimal approximation to $\{s'_k\}$,

$$\theta = \inf_{\{s_k\} \in K_M} \operatorname*{dist}_M(\{s_k\}, \{s'_k\}), \qquad [5]$$

where

$$\operatorname*{dist}_M(\{s_k\}, \{s'_k\}) = \left[\frac{1}{M} \sum_{k=1}^{M} (s_k - s'_k)^2 \cdot w_k \right]^{1/2},$$

where, in our case, the weights (w_k) were equal and normalized to 1.

By standard convexity and compactness arguments it follows that (see Ref. (*10*)) the infimum (a) is attained, (b) is unique, and (c) is just on the boundary of the convex body K_M, i.e., $2N < M + 1$, for M-odd (*7*), and (d) by filtering, the error does not increase. All of these statements can be illustrated geometrically in particular cases, when $M = 2, 3, 4$.

For numerical convenience our filtering problem may be approximated by the following discretized version (see Appendix C for the discretization error bound):

$$s_k \cong \sum_{\alpha=1}^{N} \xi_\alpha^k \rho_\alpha,$$

$$\inf_{\rho_\alpha \in \Sigma_N} \left(\sum_{k=0}^{M} (s'_k - \sum_{\alpha=1}^{N} \xi_\alpha^k \rho_\alpha)^2 \right) = M\delta^2, \qquad [6]$$

where δ is the least-square deviation, $\xi_\alpha \in [a, b]$ are the discretization points, and Σ_N is the N-dimensional standard simplex, i.e.,

$$\Sigma_N = \{\{\rho_\alpha\} | \rho_\alpha \geq 0; \sum_{\alpha=1}^{N} \rho_\alpha = 1\}.$$

$\Sigma_N \subset R^N$, with N large enough (e.g., for $N = 3$, Σ_N is the triangle whose vertices are (1, 0, 0), (0, 1, 0), (0, 0, 1)). The ρ_α, $\alpha = \overline{1, N}$ are the reconstructed, approximated populations.

The optimization algorithm used by the authors is then a slight modification of the Fletcher–Reeves (FR) conjugate gradient method, because the optimization may proceed either in interior ($\rho_\alpha > 0$) or on the "faces" (several $\rho_\alpha = 0$) of the simplex Σ_N, which are lower dimensional (*12*). In the latter cases, we applied the conjugated gradient method, restricted to corresponding "faces," until the boundary (i.e., a new ρ_α vanishing) is attained. Then the FR algorithm is restarted at the new face, with new free variables. The procedure ends after a finite number of steps, exactly in the interior point of a face (or on a vertex), i.e., much of ρ_α are zero (only one ρ_α is nonzero, i.e., a single exponential representation).

As a stop criterion, the condition may be chosen that the Fletcher–Reeves iteration should not attain to the boundary of a given face of the simplex. In our examples, usually this part of optimization ended at a face of Σ_N with very low dimensions ($\leq$6), depending on the true spectrum of the signal and the noise.

At this stage the CONTIN package (*13*) could be used instead of the previous optimization algorithm, with the positivity condition imposed, without regularization.

After computing the infimum from Eq. [6], we obtain a representation of the form as that in Eq. [1a],

$$s_k = \sum_{\alpha=1}^{N} \rho_\alpha \xi_\alpha^k, \; k = \overline{0, M}, \qquad [7]$$

with $\rho_\alpha \geq 0$.

Remember a fundamental result from (*7*): Every sequence, from Eqs. [1a] and [1b] (or equivalently), that satisfies the positivity conditions (**R**) could be represented as Eq. [7] in an infinity of manners if $2N > M + 1$. Moreover, at least one of ξ_α may be placed everywhere, on $[a, b]$. In Eq. [7] we have at least a free parameter and the corresponding quadratic forms

are strictly positive. In our case, the sequence is on the boundary, and we can proceed on a further optimization, by refining the discretization set $\{\xi_\alpha\}$ in $[a, b]$ and keeping $\rho_\alpha \geq 0$, having as inputs the values obtained from stage 1.

III.3. The Reconstruction of the Original Signal

If we performed P measurements under the same physical conditions and filtered each of the signal sequences, then let there be $\{s_k^{(1)}\}, \ldots, \{s_k^{(p)}\}$, $k = \overline{0, M}$, the collection of signal sequences, with the associated weights $w_a > 0$, $\sum_{a=1}^{P} w_a = 1$. Denote by

$$s_k^{(a)} = \sum_{\alpha=1}^{P} \rho_\alpha^{(a)} \xi_\alpha^k, \; k = \overline{0, M}, \; a = \overline{1, P} \qquad [8]$$

the representations after filtering, which are unique as we stated previously. *This uniqueness gives the false impression of correct and stable reconstruction.* Because, as we have seen, the filtered signal is always on the boundary of K_M, irrespective of the spectrum of unperturbed, ideal, true, noiseless signal, the filtered signals separately cannot reproduce the correct behavior because the true, noiseless signal most probably is in the interior of K_M.

On general grounds, the convex (weighted) mean

$$s_{k,w} = \sum_{a=1}^{P} s_k^{(a)} w_a \qquad [9a]$$

of the signal, or

$$\rho_\alpha = \sum_{n=1}^{P} \rho_\alpha^{(a)} w_a, \qquad [9b]$$

for large P must be used, instead of separate representations given by Eq. [8].

The choice of the weight in Eq. [9a] depends only on experimental conditions. We used $w_a = 1/P$. When P is sufficiently large, the computed sequence $\{s_{k,w}\}$ will be an interior point of the set of all physically admissible sequences (i.e., all $\rho_\alpha > 0$), and at least in this respect more resembling to an unperturbed, original signal sequence, in the generic case.

IV. RECONSTRUCTION OF MEAN VALUES

As we stated in Section III.2, if the signal should satisfy the positivity conditions and if we should have no precise information on the number of terms in Eq. [1a], or worse, if we should have continuous components (as in Eq. [1b]), the reconstruction could not be performed unambiguously. In the followings we attack the reconstruction problem with more precautions; i.e., we do not suppose any extra constraints on $d\sigma(x)$ (or $d\rho(\tau)$), with the exception of Eqs. [4] and $d\sigma(x) \geq 0$ or $d\rho(\tau) \geq 0$. Next we discuss the stability of reconstruction of mean values, which generalizes those treated in Section II. Define the mean value of the function $f(x)$ as

$$I(f, \sigma) \overset{\text{Def}}{=} \int_a^b f(x) d\sigma(x) = \int_{T_{\min}}^{T_{\max}} f(\exp(-\Delta t/\tau)) d\rho(\tau), \qquad [10]$$

where f is at least a continuous function.

The word "stability" will be defined now.

IV.1. Mathematical Stability (Idealized Case)

Let us suppose that s_k ($k = \overline{0, M}$) satisfies the positivity conditions and is exact (i.e., no measuring error appears). In this case, we are interested only in the estimation error of $I(f, \sigma)$ from Eq. [10], due to the finite amount of information on s_k ($k = \overline{0, M}$), when M is finite. In Appendix D we used the fact that if $f(x)$ is continuous, the error due to nonunique reconstruction of relaxation time distribution should decrease to 0 as $M \to \infty$. This is a well-understood mathematical result, but we insert it here for the nonmathematician reader's convenience. This is the meaning of "mathematical" or "idealized" stability. Even when $f(x)$ is not continuous, we could also prove the stability under several restrictions, but we did not make use of this possibility.

IV.2. Experimental Stability (Real Case)

The problem is that many test functions $f(x)$ of high interest, namely those which are strongly peaked in the neighborhood of some points and take small values away, i.e., those which could give us localized information, despite the approximations by polynomials (from Appendix D), give rise to an error term $R_M(x)$, with

$$R_M(x) = f(x) - \sum_{k=0}^{M} p_k x^k. \qquad [11]$$

With $R_M(x)$ very small on $[a, b]$, the coefficients p_k might be very large numbers, which is a well-known fact in numerical analysis. The previous approximation (see Appendix D) in realistic cases when $s_k' = s_k + \Delta s_k$,

$$I(f, \sigma) = \int_a^b f(x) d\sigma(x) = \sum_{k=0}^{M} p_k s_k' + \int_a^b R_M(x) d\sigma(x), \qquad [12]$$

contains in fact a new error term $\Sigma\, p_k \cdot \Delta s_k$, when s_k are affected by errors. At least to our knowledge, this problem was not treated.

The elucidation of this mathematical problem is given in Appendix E.

IV.3. Practical Method for Error Estimation

Next we expose a practical method for evaluating the error. We will show that the optimally reconstructed mean value $I(f, \sigma) = \int_{T_{\min}}^{T_{\max}} f(x)d\sigma(x)$ lies between maximal and minimal values of $I(f, \sigma^a)$, where σ^a ($a = \overline{1, P}$) are the reconstructed distributions of P independent measurements, performed under the same physical and chemical conditions.

Because of the convexity of the set K_M of all possible, ideal, noiseless signals and of the linear dependence on $d\sigma$ of the mean value of $I(f, \sigma)$ (from Eq. [10]), the extreme values of $I(f, \sigma)$, with $\sigma \in \Sigma'$, where Σ' is some convex subset of the simplex Σ_N, are attained in the extreme points of Σ'. In our case, this means that the extreme values of $I(f, \sigma)$ are attained on some of the reconstructed populations $\{\rho_\alpha^a\}$ for some a.

In our case, $\Sigma' = \text{conv}(\sigma^a)$ (according to Eq. [11]) where σ^a are the singular distributions from Eq. [8]:

$$s_k^{(a)} = \int_a^b x^k d\sigma^{(a)} = \sum_{\alpha=1}^{N} \rho_\alpha^{(a)} \xi_\alpha^k, \; a = \overline{1, P}, \; k = \overline{1, M}.$$

Therefore

$$\sigma^a(x) = \sum_{\alpha=1}^{N} \rho_\alpha^{(a)} \theta(x - \xi_\alpha),$$

where $\theta(x)$ is the Heaviside function.

Thus

$$I_- \le \int_a^b f(x)d\sigma(x) \le I_+,$$

where

$$I_+(f) = \max_{a=\overline{1,P}} \int_a^b f(x)d\sigma^{(a)}$$

$$= \max_{a=\overline{1,P}} \sum_{\alpha=1}^{N} \rho_\alpha^{(a)} f(\xi_\alpha) = \max_{a=\overline{1,P}} I(f, \sigma^a)$$

$$I_-(f) = \min_{a=\overline{1,P}} \int_a^b f(x)d\sigma^{(a)}$$

$$= \min_{a=\overline{1,P}} \sum_{\alpha=1}^{N} \rho_\alpha^{(a)} f(\xi_\alpha) = \min_{a=\overline{1,P}} I(f, \sigma^a),$$

and the error of the mean value $I(f)$

$$I(f) = \sum_{a=1}^{P} w_a \sum_{\alpha=1}^{N} \rho_\alpha^{(a)} f(\xi_\alpha) = \sum_{a=1}^{P} w_a I(f, \sigma^a)$$

is bounded by $|\Delta I(f)| \le I_+(f) - I_-(f)$.

In order to have a clear, global view, we usually computed a family of mean values with variable x_0 or T_0 of the form

$$M_x(x_0) = \int_a^b f\left(\frac{x - x_0}{b - a} \cdot R_x\right) d\sigma(x)$$

or

$$M_T(T_0) = \int_a^b f\left(\frac{\tau - T_0}{T_{\max} - T_{\min}} \cdot R_T\right) d\rho(\tau),$$

when R_x or R_T are the resolution factors in x or T variables.

The $M_x(x_0)$ or $M_T(T_0)$, when $f(x)$ is a positive function, peaked near 0.

We study the reproductibility of the curves $M_T(x_0)$ versus x_0, respectively $M_T(T_0)$ versus T_0, for various resolution factor values. As expected, for high R_x or R_T, the reconstruction error is very large; i.e., if we should want to localize some components (low Γ), the error, in mean value increases. This is similar to Heisenberg's uncertainty relations, but its origin lies in the multiplicity of solutions of the finite-input (Markov) momentum problem and is not related to quantum physics of NMR.

IV.4. Relation to Other Methods

Our method differs from methods used previously (*13, 14*) by its objective: instead of trying to reconstruct the distribution function $d\rho(\tau)$ from Eq. [1b], which, as stated before, is nonunique, in rigorous sense, we reconstruct the mean values $I(f, \sigma)$ from Eq. [10] with $f(\tau)$ smooth. In some cases this reconstruction can be done directly (see Section II), but in general, we use some approximate reconstruction of $d\sigma(x)$ or $d\rho(\tau)$, *as an intermediate technical step.* Note that the computation of $I(f, \sigma)$ has a healing, stabilizing effect. It is possible that by applying our "smoothing" $I(f, \sigma)$ to the output of previous methods (*13, 14*), we will obtain more stable values.

From our previously rigorous treatment a few main conclusions emerge:

A. The measured signal never fulfills the positivity conditions.

B. The filtered signal is on boundary of the set of all admissible, noiseless signal sequences K_M. If we do not know a priori where the true signal is, we must perform a large number of measurements, under the same physical conditions,

to obtain a sequence that shares the qualitative property of the true signal—the fact that it is in inside of K_M.

C. Even if we have a signal inside of K_M, its reconstruction is impossible. Trying to write programs with discretization or regularization (*13*), we in fact impose some new, unproved assumptions. When the regularization is removed progressively or the discretization is refined, the above mentioned nonuniqueness shows up in the slowing down or numerical instabilities and in the dependence of the final results on the starting point of minimization.

D. These nonuniquenesses may be irrelevant for mean values (see, e.g., Section II, where the mean values were reconstructed without nonlinear filtering, or Sections IV.1 and IV.2, where the mean values can be approximated by polynomial approximation of smooth function, without the reconstruction of relaxation time). Consequently, our approach adds two new steps to the signal processing: one, computation of mean values and, two, study of the stability of mean values (see Section IV.3). Other algorithms (most preferably CONTIN, with positivity restriction imposed) can be used as preliminary steps, but these, although useful, steps are important only for error reducing. The mean values can be computed directly (see Sections IV.1 and IV.2) in the low-noise cases.

E. Linear methods of reconstruction (that do not impose positivity restriction **R**) in virtue of statements of Appendix B necessarily give rise to unphysical negative values of the reconstructed populations, in the case of the inversion of Laplace transform.

F. The success and apparent stability of previous reconstruction methods can be explained by:

(1) The (eventually hidden or explicit, in the case of CONTIN) numerical implementations of some new, unproved regularizing restrictions (e.g., smoothness of relaxation time distribution function, fixed number of relaxation times); and

(2) The fact that the true signal does not obey (**R**) and the reconstructed signal, being on the boundary of K_M, is unique. *But this is a false impression of stability and uniqueness, unless we have no extra information that the true signal is really on the boundary of* K_M.

We remind that another method for treating unstable problems (*8*) consists of looking for solutions in a more restricted class, e.g., in our case imposing smoothness on the relaxation time distribution function. Then the ouptut will be very similar qualitatively to the output of our approach: a convoluted (with a smooth function) relaxation time distribution function, despite being numerically different, due to the nonlinearity of filtering. In our approach, we use only the positivity conditions. The regularizing effects of smoothing by convolution in our approach are rigorously proved.

V. NUMERICAL SIMULATION

We applied the mathematical method described above to a series of simulated time-domain signals. The series of simulated time-domain signals was obtained as follows: The signal of the simulated NMR time domain s'_k at time $t_k = \Delta t \cdot k$ is described by

$$s'_k = s(k\Delta t) + \Delta s_k,$$

$$s_k = s(\Delta t \cdot k) = \int_{T_{\min}}^{T_{\max}} \exp(-\Delta t \cdot k/\tau) d\rho(\tau)$$

or

$$s_k = \sum_i n_i \exp(-\Delta t \cdot k/T_i),$$

in case we choose a discrete spectrum, with known n_i and T_i, $k = \overline{0, N}$ similar to Eq. [1a], where n_i, T_i, and consequently s_k are known and Δs_k are the Gaussian noise terms generated by random number generator.

The function f was chosen of the class $C^1(T_{\min}, T_{\max})$, i.e., continuously differentiable, defined as

$$f(t) = \begin{cases} 0 \text{ if } |t| > \Gamma \\ \left(1 - \left(\dfrac{t}{\Gamma}\right)^2\right)^2 \quad \text{if} \quad |t| \le \Gamma' \end{cases}, \qquad [13]$$

where

$$\Gamma = \frac{T_{\max} - T_{\min}}{R}$$

and R ("resolution factor") is a measure of the resolution.

The normalization $f(0) = 1$ is chosen so that when R should increase, the graph of the function

$$F(T) = \int_{T_{\min}}^{T_{\max}} f(t - T) d\rho(t)$$

$$= f \otimes \frac{d\rho(t)}{dt} = I(f(t - T), \rho(t)), \qquad [14a]$$

where $\otimes$ stands for convolution product, or for a discrete spectrum

$$F(T) = \sum_{\alpha=1}^{N} f(t_\alpha - T)\rho_\alpha, \qquad [14b]$$

would approximately reproduce the discrete distribution of populations n_i, at relaxation times T_i. As we could expect,

TABLE 1
Numerical Results for Numerical Simulation

SNR (dB)		40	60	66.5	70	80
$N = 2$	R_{max} (for $\delta_2 \leq 0.01 = \delta_{2,max}$)	3	6	6	6	7
($T_1 = 500$, $T_2 = 1000$ ms)	R_{max} (for $\delta_2 \leq 0.05 = \delta_{2,max}$)	12	24	25	25	29
	R_{max} (for $\delta_2 \leq 0.1 = \delta_{2,max}$)	24	44	46	46	52
$N = 3$	R_{max} (for $\delta_2 \leq 0.01 = \delta_{2,max}$)	1	2	3	3	5
($T_1 = 500$, $T_2 = 1000$, $T_3 = 1500$ ms)	R_{max} (for $\delta_2 \leq 0.05 = \delta_{2,max}$)	2	4	7	10	19
	R_{max} (for $\delta_2 \leq 0.1 = \delta_{2,max}$)	3	6	14	20	37
$N = 4$	R_{max} (for $\delta_2 \leq 0.01 = \delta_{2,max}$)	1	2	2	3	4
($T_1 = 200$, $T_2 = 650$, $T_3 = 1100$,	R_{max} (for $\delta_2 \leq 0.05 = \delta_{2,max}$)	2	3	4	5	9
$T_4 = 1650$ ms)	R_{max} (for $\delta_2 \leq 0.1 = \delta_{2,max}$)	3	4	6	9	18

when Γ decreases, R increases, so the error in the reconstruction of $F(T)$ increases. Note that when we expect continuous or multiple relaxation time signals, the dirac–delta normalization is preferred:

$$\int_{T_{min}}^{T_{max}} f(t)dt = 1.$$

But we must enlighten the more instructive (despite it being unusual and unphysical) x representation, which for a T_2 spectrum reduces to

$$s(k\Delta t) = \sum_{i=1}^{N} n_i x_i^k = \int_a^b x^k d\sigma(x), \quad \text{with} \quad x_i = \exp\left(-\frac{\Delta t}{T_i}\right).$$

Depending on whether x_i and x_{i+1} are separated or close, we can recover the distribution more or less exactly. We can obtain another type of mean value by choosing instead of Eq. [13]

$$f(t) = \frac{1}{2} - \frac{1}{\pi} \operatorname{arctg} \frac{t}{\Gamma}, \tag{13a}$$

where

$$\Gamma = \frac{T_{max} - T_{min}}{R}$$

or

$$f(t) = \frac{e^{t/\Gamma}}{e^{t/\Gamma} + e^{-t/\Gamma}},$$

i.e., smoothed Heaviside-like functions.

The noise contribution of each data point is a Gaussian distribution with a mean equal to 0 and a standard deviation equal to σ_{noise}. The noise contributions of successive data points are noncorrelated.

The signal-to-noise ratio (SNR) is defined by

$$\text{SNR} = 10 \log_{10}\left(\frac{\text{signal power}}{\text{noise variance}}\right) = 10 \log_{10}\left(\frac{\sum_{n=0}^{M} s^2(n \cdot \Delta t)}{2(M+1)\sigma_{noise}^2}\right). \tag{15}$$

We use the expression of δ_2

$$\delta_2 = \left[\frac{\|F - F'\|_{L^2}^2}{\frac{\|F\|_{L^2}^2 + \|F'\|_{L^2}^2}{2}}\right]^{1/2} \cong \left[\frac{\sum_{k=1}^{N'} |F(t_k) - F'(t_k)|^2}{\sum_{k=1}^{N'} \frac{((F(t_k))^2 + (F'(t_k))^2)}{2}}\right]^{1/2}, \tag{16}$$

where N' is the number of discretization points, $F(T)$ is computed from Eq. [14b], from known n_i and T_i, and $F'(T)$ is computed as follows: add to $s(t_k)$ (where $s(t_k)$ is the "ideal signals" from known n_i and T_i in Eq. [1a]) a Gaussian noise and compute $F'(T)$ by our method using Eq. [14b]. With the expression of δ_2 from Eq. [16], we are able to characterize the reconstruction relative error. In the simulation process, the signal was constructed using Eq. [1a] ($2 \leq N \leq 4$).

The values of T_i were chosen between $T_{min} = 0$ ms (when we have no extra information) and $T_{max} = 2000$ ms $\gg \Delta t =$ 8 ms with the same peak amplitude n_i. The upper bound of R is 100. The reconstruction program does not use N from Eq. [1a] as input.

In Table 1 we insert the maximum of the resolution factor (R_{max} from Eq. [13]) calculated at the various SNR values and for three thresholds of $\delta_{2,max}$, for $R \leq R_{max}$, $\delta_2 \leq \delta_{2,max}$.

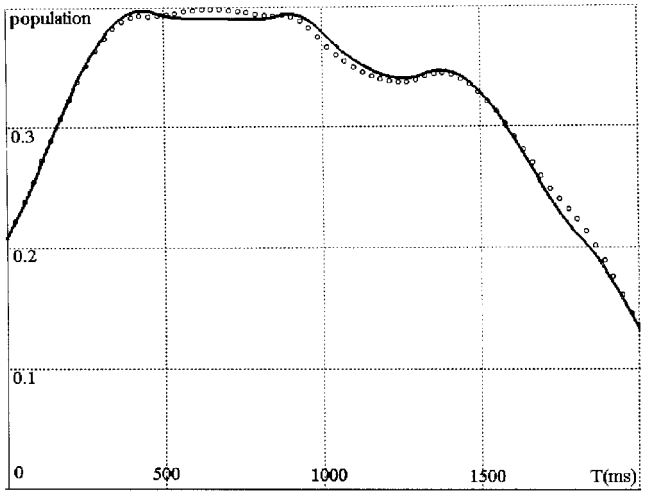

FIG. 1. The convolution of T_2 distribution with a smoothed dirac-delta-like function, with known (open circles) and reconstructed distribution (solid line) in the case of $N = 4$, $R = 3$.

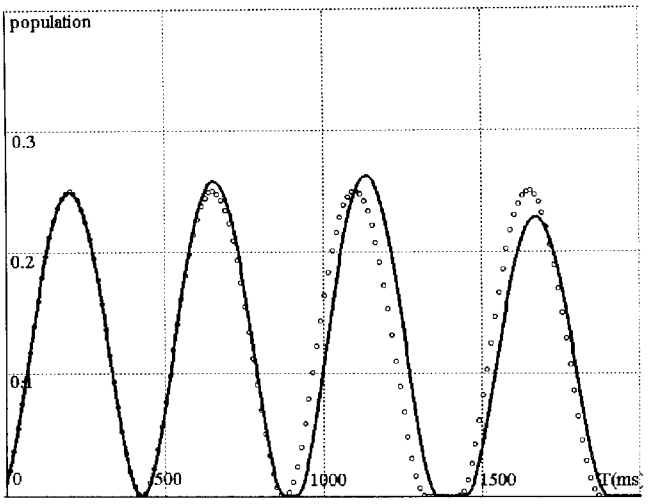

FIG. 3. The convolution of T_2 distribution with a smoothed dirac-delta-like function, with known (open circles) and reconstructed distribution (solid line) in the case of $N = 4$, $R = 9$.

In Figs. 1, 2, and 3 are represented the convolution of T_2 distribution with a smoothed dirac-delta-like function (Eq. [14b]), with known (open circles) and reconstructed distribution (solid line) at $R = 3$, 5, and 9, for the signal obtained by the sum of equally populated four exponentials.

We can evaluate (from Table 1) the confidence degree of the numerical result, which is similar to a low-resolution NMR experiment.

It is possible also to use another function, the "staircase" function-type Eq. [13a] for the convolution of T_2 distributions with a smoothed Heaviside-like function, with known and reconstructed distribution.

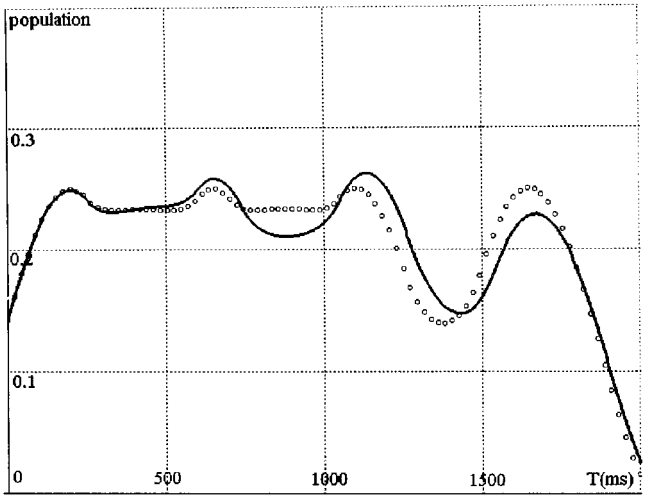

FIG. 2. The convolution of T_2 distribution with a smoothed dirac-delta-like function, with known (open circles) and reconstructed distribution (solid line) in the case of $N = 4$, $R = 5$.

Despite the localization not being so clear, these functions are more stable to experimental fluctuations.

VI. EXPERIMENTAL SIMULATION

The NMR measurements were performed with a pulsed ^{1}H NMR Aremi-78 spectrometer (manufactured by the Institute of Physics and Nuclear Engineering, Bucharest-Magurele, Romania) at a frequency of 25 MHz. The temperature was controlled up to a precision of ± 0.2°C by airflow over an electrical resistance, using the variable temperature unit attached to the spectrometer. The temperature in the sample was measured with a thermocouple connected to a microprocessor thermometer. All NMR measurements were carried out at 25 ± 0.2°C.

For T_2 estimations, we used a series of standard Carr–Purcell–Meiboom–Gill (CPMG) sequences (*15*) with variable 90°–180° interpulse delays ($\tau = 0.10$–12 ms, adapted to be distinct among samples), 1024 points in common, 10 scans, and a repetition delay (RD) of 10 s. These parameters allow for a good characterization of the slow relaxing component. The CPMG T_2 decay was measured by sampling the height of the echoes.

For experimental simulation we have used different solutions of extinctor substance for water protons $MnCl_2$.

We used two different concentrations and twice-distilled water. First, we measured the relaxation time T_2 for every sample using our many-exponential fitting program and validated these by another nonlinear regression program based on the Marquardt algorithm (*16*). As expected, we have obtained in every case one exponential relaxation centered at 40, 400,

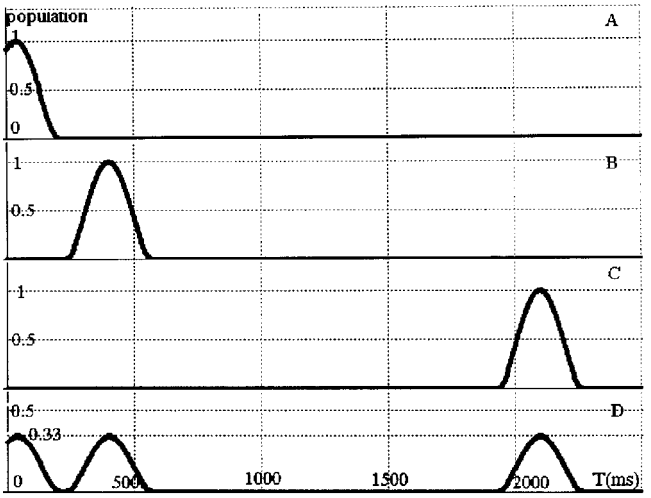

FIG. 4. (A, B, and C) The reconstructed single convolution centered at 40, 400, and 2100 ms, respectively; (D) the reconstructed convolution from the sum of three exponentials. All the convolutions are drawn at $R = 15$.

and 2100 ms (see Figs. 4A, 4B, and 4C, respectively). Next, we analyzed the combinations of these three samples. An equal quantity of each solution was enclosed in the capillary tubes, and we analyzed them together. Thus, we obtained an experimental signal composed of the sum of three exponentials. The experimental signal has an SNR near to 50 dB. This signal was fitted by our program. As we expected, we obtained three separate distributions near to the specific distributions determined in stage one (centered at 42.5, 386, and 2105 ms) (see Fig. 4D). If we admit that the three distributions from the first stage are reference signals for the distribution obtained in stage two, we could calculate $R_{\max}$ for different δ_2 (see Table 2).

VII. PRACTICAL RECIPE

0. Normalize the signal $s_k = s(k\Delta t)$, to $s(0) = s_0 = 1$ and retain old value of $s(0)$ for further application.

1. Select a discretization of time T_α or $x_\alpha = \exp(-\Delta t/T_\alpha)$ variable $\xi_\alpha = \exp(-\Delta t/T_\alpha)$, where $T_{\min} < T_\alpha \leq T_{\max}$, such that the discretization error ϵ_N from Appendix C should be much lower than the experimental error (see the recipe at end of Appendix C).

2. For one or, better, several signal sequences perform the least-square fit: if $s_k = s(k\Delta t)$ is the signal, find $\rho_\alpha \geq 0$ which gives, in the above discretized approximation, the best fit,

$$s_k \cong \sum_{\alpha=1}^{N} \rho_\alpha \exp(-k\Delta t/T_\alpha) = \sum_{\alpha=1}^{N} \rho_\alpha \xi_\alpha^k,$$

$$k = \overline{0, M}, \quad \text{or} \quad k = \overline{1, M} \quad \text{and} \quad \sum_{\alpha=1}^{N} \rho_\alpha = 1,$$

and store these values of ρ_α. (CONTIN with regularization and positivity condition imposed can be used.)

2′. Repeat step 2 for various measurements performed under the same phsyical conditions.

3. Select some smooth functions $f(t)$ (e.g., Eq. [13]) and compute for T_α (step 1) and ρ_α (step 2–2′) the graph $(F(T), T)$ of the function $F(T)$ $(T_{\min} < T \leq T_{\max})$ given by

$$F(T) = \sum_{\alpha} \rho_\alpha \cdot f(T - T_\alpha).$$

4. Study the error propagation from various signals (step 2′) to the graph of $F(T)$. In the case of poor reproducibility, decrease the resolution factor R, or select a new, much smoother function f.

VIII. CONCLUSIONS

We proved that the straightforward functional analytical approach to the NMR signal treatment could provide a clear setting of the questions about the possibility of obtaining numerically stable results on T_2 distribution. Despite the fact that it is impossible to exactly localize separated exponential terms, the mean value of the distribution functions can be reconstructed and generates, as a byproduct, a partial localization of the T_2 terms, even in the presence of noise. Our numerical examples suggest that a partial localization of at least 10% is always possible, even under the experimental conditions of SNR $\approx$ 50–70 dB. In terms of functional analysis, this kind of reconstruction of mean values is termed as "weak convergence."

The objectives of future investigations are twofold: mathematical and experimental. From the mathematical point of view, we must solve the problem stated at the end of Appendix E, in order to speed up the computations related to the error estimation. From the experimental point of view, it is important to work out the standardization of the functions whose mean values we compute, which depends on the physical, chemical, and biological origins of the samples investigated.

TABLE 2
Numerical Results for Experimental Simulation

SNR (dB)	50
$R_{\max}$ (for $\delta_2 \leq 0.01 = \delta_{2,\max}$)	2
$R_{\max}$ (for $\delta_2 \leq 0.05 = \delta_{2,\max}$)	6
$R_{\max}$ (for $\delta_2 \leq 0.1 = \delta_{2,\max}$)	15

APPENDIX A

Direct Calculation of Some Mean Values without Reconstruction of the T_2 Distribution Function

The correctness for the choice of the cutoff parameter in Eq. [3] may be verified by the Hölder inequalities

$$\left| \int \prod_{i=1}^{n} f_i d\sigma \right| \leq \prod_{i=1}^{n} \left(\int f_i^{p_i} d\sigma \right)^{1/p_i}, \sum_{i=1}^{n} \frac{1}{p_i} = 1, \; 1 \leq p_i,$$

which give, if $\beta = \sum_{i=1}^{n} \beta_i$,

$$\langle T^{\beta} \rangle \leq \prod_{i=1}^{n} \langle T^{\beta_i p_i} \rangle^{1/p_i}, \; p_i \geq 1, \; \sum_{i=1}^{n} \frac{1}{p_i} = 1. \qquad [A1]$$

We remark that values $\langle T^{\alpha} \rangle$, $\alpha > 0$, are more sensitive to large relaxation times. Nevertheless, we can roughly estimate the contribution of lower relaxation times in a stable way too. We obtain (using Eq. [2])

$$\begin{aligned} \int_0^{\infty} e^{-t/T_0} s(t) dt &= \int_{T_{\min}}^{T_{\max}} d\sigma(\tau) \frac{\tau \cdot T_0}{\tau + T_0} \\ &= T_0 - T_0^2 \int_{T_{\min}}^{T_{\max}} \frac{d\sigma(\tau)}{\tau + T_0} \\ &= T_0 - T_0^2 \left\langle \frac{1}{\tau + T_0} \right\rangle_{\tau}. \end{aligned}$$

Thus

$$\begin{aligned} \left\langle \frac{1}{\tau + T_0} \right\rangle_{\tau} &= \int_{T_{\min}}^{T_{\max}} \frac{d\sigma(\tau)}{\tau + T_0} = \frac{1}{T_0} \left(1 - \frac{1}{T_0} \int_0^{\infty} e^{-t/T_0} s(t) dt \right) \\ &\cong \frac{1}{T_0} \left(1 - \frac{1}{T_0} \int_0^{\Lambda} e^{-t/T_0} s(t) dt \right). \qquad [A2] \end{aligned}$$

Differentiating Eq. [3] with T_0, we can compute $\langle (1/(\tau + T_0))^2 \rangle_{\tau}$ and the dispersion of $1/(\tau + T_0)$:

$$\left\langle \frac{1}{(\tau + T_0)^2} \right\rangle_{\tau} = \frac{1}{T_0^2} + \frac{1}{T_0^3} \int_0^{\infty} \left(\frac{t}{T_0} - 2 \right) e^{-t/T_0} s(t) dt. \qquad [A3]$$

Then

$$\begin{aligned} \sigma_{T_0}^2 &\overset{\text{Def}}{=} \left\langle \left(\frac{1}{\tau + T_0} - \left\langle \frac{1}{\tau + T_0} \right\rangle_{\tau} \right)^2 \right\rangle_{\tau} \\ &= \left\langle \left(\frac{1}{\tau + T_0} \right)^2 \right\rangle_{\tau} - \left\langle \frac{1}{\tau + T_0} \right\rangle_{\tau}^2. \qquad [A4] \end{aligned}$$

Then σ_{T_0} provides an error estimation of the displaced by T_0 harmonic mean T_{h}.

APPENDIX B

Upper Bound of the Probability That the Experimental Signal Should Be Mathematically Correct

Consider the less restrictive case $T_{\min} = 0$ and $T_{\max} = \infty$. Let $s_1, \ldots, s_M$, a random sequence with $s_0 = 1$, $0 \leq s_k \leq 1$, $k = \overline{1, M}$, be uncorrelated and uniformly distributed. Denote by D_M the probability that this sequence be a true, idealized NMR signal, i.e., could be written like Eq. [1b]. We translate a result of (*17*) in NMR terminology. According to (*17*) this probability D_M is

$$D_M = \prod_{k=1}^{M} \left[\frac{((k-1)!)^2}{(2k-1)!} \right], \qquad [B1]$$

where M is the number of equidistant samples.

In mathematical terms, this is the probability that $(s_0, s_1, \ldots, s_M) \in K_M$ (or $s_0 = 1$ and obeys (**R**)). Then, if instead of ideal signals $(s_1, \ldots, s_M)$ we should have one distributed according to probability distribution function $f(s_1, \ldots, s_M)$, the probability of obtaining a physically admissible (obeying restriction **R**) signal would be

$$P_M = \int_{K_M} f(s_1, \ldots, s_M) ds_1, \ldots, ds_M \leq \bar{f} D_M, \qquad [B2]$$

where $\bar{f}$ is the maximal value of $f(s_1, \ldots, s_M)$. For a Gaussian distribution, with dispersion σ_1

$$\bar{f} = 1/(\sqrt{2\pi}\sigma_1)^M. \qquad [B3]$$

Taking an overoptimistic value $\sigma_1 = 10^{-6}$ from Eqs. [B1], [B2], and [B3] we find that for, e.g., $M = 6$, $P_M < 2 \times 10^{-27}$, and is "cosmologically small" for higher M. If $T_{\min}$ or $T_{\max}$ are known, this probability will be smaller.

APPENDIX C

The Discretization Error Estimated

Readers interested in applications can read only the final recipe, without the forthcoming proof. By definition, the K_M set can be viewed as the smalleset convex body in R^M, which contains the curve Γ: $[a, b] \xrightarrow{f} R^M$, given by $x \to \{x^k\}$, $k = \overline{1, M}$. Consequently, we can approximate the curve Γ by a general polygonal curve Γ^N, whose vertices lie on Γ, and K_M by $K_M^N \subset K_M$ where K_M^N is the convex hull of the points' polygonal line Γ^N.

We denote by $\xi_\alpha \in [a, b]$ the N points. We also denote by $\mathbf{s}_\alpha$, $\alpha = \overline{1, N}$, the vectors from R^M, $\mathbf{s}_\alpha = \{s_{\alpha,k}\}$, with $s_{\alpha,k} = \xi_\alpha^k$.

Then K_M^N is the convex hull of the points $\{\mathbf{s}_\alpha\}$, $\alpha = \overline{1, N}$, $K_M^N \subset K_M$ and for ξ_α equally spaced,

$$\bigcup_{N=M_0}^{\infty} K_M^N = K_M.$$

Then we can compute δ_N ($\geq \delta$) (the discretization error):

$$\delta_N = \inf_{\{s_k\} \in K_M^N} \operatorname{dist}(\{s_k\}, \{s_k'\}),$$

and we have for $s_k \in K_M^N$

$$s_k = \sum_{\alpha=1}^{N} \rho_\alpha \xi_\alpha^k,\ \rho_\alpha \geq 0,\ s_0 = \sum_{\alpha=1}^{N} \rho_\alpha = 1.$$

The approximation error can be bounded readily. We denote

$$\epsilon_N = \max_{k=1,M} \max_{\alpha=1,N-1} \Delta_\alpha^{(k)}, \qquad \text{[C1]}$$

where $\Delta_\alpha^{(k)}$ is the maximal error in approximating on $[\xi_\alpha, \xi_{\alpha+1}]$ the function x^k by the linear function

$$\varphi(x) = \xi_\alpha^k + \frac{\xi_{\alpha+1}^k}{\xi_{\alpha+1} - \xi_\alpha}(x - \xi_\alpha),$$

which is a segment of the polygonal curve Γ^N, the approximations of Γ joining two neighbor vertices.

The error induced by discretization is less than ϵ_N.

$\Delta_\alpha^{(k)}$ can be computed easily:

$$\Delta_\alpha^{(k)} = \sup_{\lambda \in [0,1]} (\lambda \xi_\alpha^k + (1 - \lambda)\xi_{\alpha+1}^k - (\lambda \xi_\alpha + (1 - \lambda)\xi_{\alpha+1})^k) \qquad \text{[C2a]}$$

or

$$\Delta_\alpha^{(k)} = \lambda^* \xi_\alpha^k + (1 - \lambda^*)\xi_{\alpha+1}^k - (\lambda^* \xi_\alpha + (1 - \lambda^*)\xi_{\alpha+1})^k. \qquad \text{[C2b]}$$

We notice that λ^* is given by

$$\lambda^* \xi_\alpha^k + (1 - \lambda^*)\xi_{\alpha+1}^k = \left(\frac{\xi_{\alpha+1}^k - \xi_\alpha^k}{k(\xi_{\alpha+1} - \xi_\alpha)}\right)^{1/(k-1)} \qquad \text{[C3]}$$

or

$$\lambda^* = \left[\left(\frac{\xi_{\alpha+1}^k - \xi_\alpha^k}{k(\xi_{\alpha+1} - \xi_\alpha)}\right)^{1/(k-1)} - \xi_{\alpha+1}^k\right] \Big/ (\xi_\alpha^k - \xi_{\alpha+1}^k), \qquad \text{[C4]}$$

and ϵ_N can be computed exactly.

We choose $\xi_k = \exp(-\Delta t/T_k)$, where T_k are uniformly distributed between $T_{\min}$ and $T_{\max}$, and for $N = 350$, $M = 230$, ϵ_N is less than 10^{-4}.

The recipe is to select a sequence of discretization points T_k ($T_{\min} \leq T_k \leq T_{\max}$), compute $\xi_k = \exp(-\Delta t/T_k)$, compute λ^* from Eq. [C4], compute $\Delta_\alpha^{(k)}$ from Eq. [C2b], and from Eq. [C1] compute the discretization error ϵ_N.

APPENDIX D

Proof of Stability in the Noiseless Case

We use the fact that, by the Weierstrass theorem, a continuous function can be approximated by polynomials. Consider a sequence of noiseless signal:

$$s_k = s(k\Delta t) = \int_{T_{\min}}^{T_{\max}} \exp(-k\Delta t/T)\, d\rho(T) = \int_a^b x^k d\sigma(x);\ k = \overline{0, M}.$$

If s_k obeys (**R**), it is well known, from the classical momentum problem, that for finite M there are an infinity of distributions $d\rho(T)$ or $d\sigma(x)$. Moreover, there are some representations

$$s_k = \sum_{i=1}^{C} n_i \exp(-k\Delta t/T_i) = \sum_{i=1}^{C} n_i \xi_i^k$$

with $2C > M + 1$, where some of T_i may be placed everywhere on $[T_{\min}, T_{\max}]$ or ξ_i on $[a, b]$ (canonical representation). Nevertheless, if $\varphi(\tau)$ ($T_{\min} \leq \tau \leq T_{\max}$) or $f(x)$

($a \le x \le b$) are continuous functions, then for sufficiently large M the integrals (mean values) $I(f, \sigma) = \int_a^b f(x)d\sigma(x)$, or equivalently $J(\varphi, \rho) = \int_{T_{\min}}^{T_{\max}} \varphi(\tau)d\rho(\tau)$, have only a slight dependence on $d\sigma(x)$. This happens because if some T_k are "misplaced," the corresponding n_i will be small (e.g., bounded by R. Nevanlinna "maximal mass" function (*7*)). Because of the equivalence of momentum and NMR reconstruction problem, we will focus on $I(f, \sigma)$. The precise statement is

Let $s_k = \int_a^b x^k d\sigma(x) = \int_a^b x^k d\sigma'(x)$, $k = \overline{1, M}$ be two distinct reconstructions, and $I'(f, \sigma) = \int_a^b f(x)d\sigma'(x)$. If $f(x)$ is continuous on $[a, b]$ then $I(f, \sigma) - I'(f, \sigma) \to 0$ as $M \to \infty$.

Proof. By Weierstrass theorem, there exists polynomials $P_M(x)$ that uniformly approximate $f(x)$:

$$f(x) - P_M(x) = R_M(x) = \text{error} \qquad \text{[D1]}$$

and

$$\sup_{s\in[a,b]} |R_M(x)| \overset{\text{Def}}{=} \epsilon_M \to 0 \quad \text{as} \quad M \to \infty. \qquad \text{[D2]}$$

Write $P_M(x) = \sum_{k=0}^M p_k x^k$; thus

$$\int_a^b P_M(x)d\sigma(x) = \int_a^b P_M(x)d\sigma'(x) = \sum_{k=0}^M s_k p_k. \qquad \text{[D3]}$$

Thus, the error $|\Delta I(f, \sigma)|$ is bounded by

$$\begin{aligned} |\Delta I(f, \sigma)| &= \left| \int_a^b f(x)d\sigma(x) - \int_a^b f(x)d\sigma'(x) \right| \\ &= \left| \int_a^b (P_M(x) + R_M(x))d\sigma(x) \right. \\ &\qquad \left. - \int_a^b (P_M(x) + R_M(x))d\sigma'(x) \right| \\ &= \left| \int_a^b R_M(x)d\sigma(x) - \int_a^b R_M(x)d\sigma'(x) \right| \\ &\le \int_a^b |R_M(x)|d\sigma(x) + \int_a^b |R_M(x)|d\sigma'(x). \end{aligned}$$

We have successively used Eqs. [D1] and [D2] and the fact that $d\sigma(x), d\sigma'(x) \ge 0$, and the next using Eq. [D3]:

$$\begin{aligned} |\Delta I(f, \sigma)| &\le \epsilon_M \left(\int_a^b d\sigma(x) + \int_a^b d\sigma'(x) \right) \\ &= \epsilon_M \cdot 2s_0 \to 0 \text{ (by Eq. [D2]).} \end{aligned}$$

APPENDIX E

Stability in Experimental Situations

We denote by $\sigma'^2_M = \sum_{k=1}^M (\Delta s'_k)^2$ the estimated mean-square error and let $\sigma_M \ge \sigma'_M$ be an error bound. We will give a definition of experimental stability by requiring that if the number of data M increases and the mean-square experimental error bound σ_M decreases to 0, then the reconstruction error of $I(f)$ should be small.

DEFINITION. A reconstruction method of $I(f, \sigma)$ is σ_M-*experimentally stable* (with $\lim_{M\to\infty} \sigma_M = 0$) if the reconstruction error $(\Delta I)_M \to 0$.

Then we have the following:

THEOREM. *Let $f \in C^1[a, b]$ and $P_M(x)$ be a polynomial of $M - 1$ degree which realizes the infimum*

$$\inf_{P_M(x)} \int_a^b (f'(x) - P_M(x))^2 dx, \; P_M(x) = \sum_{k=1}^M b_k x^{k-1}.$$

We denote that $C_M = (\sum_{k=1}^M (b_k/k)^2)^{1/2}$.

If $\sigma_M \cdot C_M \to 0$, then the reconstruction is σ_M-experimentally stable.

Proof. Let $f(x) = R_M(x) + \sum_{k=1}^M p_k x^k$, $I(f, \sigma) = \int_a^b f(x)d\sigma(x)$, and assuming that in Eqs. [11] and [12], $f(x)$ is continuously differentiable, integrating by parts we obtain, from Eq. [12]

$$\begin{aligned} I(f, \sigma) = \sum_{k=0}^M p_k s_k + R_M(b)\sigma(b) - R_M(a)\sigma(a) \\ - \int_a^b R'_M(x)\sigma(x)dx. \end{aligned} \qquad \text{[E1]}$$

We can choose $\sigma(a) = 0$ and $R_M(b) = 0$. Then $|\sigma(x)| \le 1$ ($s_0 = 1$). The error is bounded by

$$|\Delta I(f, \sigma)| \le \sum_{k=1}^M |p_k||\Delta s_k| + \int_a^b |R'_M(x)|\sigma(x)dx, \qquad \text{[E2]}$$

and by the Schwartz inequality

$$|\Delta I(f,\sigma)| \le \Big(\sum_{k=1}^{M} p_k^2\Big)^{1/2}\Big(\sum_{k=1}^{M} \Delta s_k^2\Big)^{1/2} + (b-a)^{1/2} \times \left(\int_a^b (R'_M(x))^2(\sigma(x))^2 dx\right)^{1/2}. \quad \text{[E3]}$$

If we define $p_k \cdot k = b_k$, then

$$|\Delta I(f,\sigma)| \le \left(\sum_{k=1}^{M}\left(\frac{b_k}{k}\right)^2\right)^{1/2} \cdot \sigma_M + \sqrt{(b-a)} \times \left(\int_a^b \Big(f'(x) - \sum_{k=1}^{M} b_k x^{k-1}\Big)^2 dx\right)^{1/2}. \quad \text{[E4]}$$

Thus $|\Delta I(f,\sigma)| \le C_M \cdot \sigma_M + \sqrt{(b-a)} \cdot \inf_{P_M} \int_a^b (f'(x) - P_M(x))^2 dx = C_M \cdot \sigma_M + \sqrt{(b-a)} \cdot \delta_M$. But because $f' \in C^1[a,b]$, $\delta_M \to 0$ when $M \to \infty$, which completes the proof.

We remark that this is only a sufficient condition. To obtain the best bound on $\Delta I(f,\sigma)$ from Eq. [E4], using the inequality $a + b \le \sqrt{2(a^2+b^2)}$ we obtain

$$\left(\frac{\Delta I(f,\sigma)}{2}\right)^2 \le \sigma_M^2 \cdot \sum_{k=1}^{M}\left(\frac{b_k}{k}\right)^2 + (b-a)\cdot \Big\| f'(x) - \sum_{k=1}^{M} b_k x^{k-1}\Big\|^2. \quad \text{[E5]}$$

Thus $(\Delta I(f,\sigma))^2 \le 2 \cdot \epsilon^2(M,a,b,\sigma_M)$, where

$$\epsilon^2(M,a,b,\sigma_M) = \inf_{b_k}\left(\sigma_M^2 \cdot \sum_{k=1}^{M}\left(\frac{b_k}{k}\right)^2 + (b-a) \times \int_a^b \Big(f'(x) - \sum_{k=1}^{M} b_k x^{k-1}\Big)^2 dx\right). \quad \text{[E6]}$$

The computation of $\epsilon^2(M,a,b,\sigma_M)$ from Eq. [E6] is a standard Hilbert space optimization problem, for $M \to \infty$ and a simple algebraic problem for finite M. The investigation of the whole class of functions $f(x)$, when $\epsilon^2(M,a,b,\sigma_M) \to 0$ as $M \to \infty$ is still an open problem in functional analysis.

REFERENCES

1. P. Claverie, A. Denis, and E. Yeramian, The representation of functions through the combined use of integral transforms and Padè approximants: Padè-Laplace analysis of functions as sums of exponentials, *Comput. Phys. Rep.* **9,** 247–294 (1989).
2. T. L. James, "Nuclear Magnetic Resonance in Biochemistry. Principles and Applications," Academic Press, New York (1975).
3. N. I. Ahiezer, "The Classical Momentum Problem and Related Problems of Functional Analysis," State Editor in Mathematics and Physics, Moscow (1961). [In Russian]
4. F. Riesz and B. Sz. Nagy, "Leçons d'Analyse Fonctionnelle," Akadémiai Kiadó, Budapest (1972).
5. R. Scorei, V. M. Cimpoiasu, I. Petrisor, M. Iacob, I. Brad, I. Olteanu, R. Grosescu, V. Scorei, M. Mitrut, and R. Cimpoiasu, Over all protons relaxation in the hydrated biopolymers systems by LRP-^{1}HNMR technique, *Rom. J. Biophys.* **7,** 327–337 (1997).
6. V. M. Cimpoiasu, Gy. Steinbrecher, I. Petrisor, R. Grosescu, R. Scorei, I. Brad, I. Olteanu, M. Iacob, V. Scorei, M. Mitrut, and R. Cimpoiasu, Monitoring the global proton relaxation in the heterogeneous systems by LRP-^{1}H-NMR technique, *Phys. AUC* **7,** 56–60 (1997).
7. M. G. Krein and A. A. Nudelmann, "Markov Momentum Problem and Extremal Questions," Nauka, Moskow (1973). [In Russian]
8. S. Ciulli, Stability problems in analytic continuation, *in* "Lecture Notes in Physics, Vol. 17, Strong Interaction Physics, Proceedings of International Summer Institute on Theoretical Physics in Kaiserslautern, 1972" (J. Ehlers, K. Hepp, and H. A. Weidenmuller, Eds.), Springer-Verlag, Berlin (1973), and references therein.
9. S. Ciulli and G. Nenciu, *J. Math. Phys.* **14,** 1675 (1973).
10. Gy. Steinbrecher, On the optimization of the variational Monte-Carlo calculations, *Phys. AUC* **8,** 89–93 (1998).
11. Gy. Steinbrecher, Monte-Carlo algorithm for few-body spectroscopy, *Phys. AUC* **2–3,** 98–105 (1993).
12. R. Fletcher and C. M. Reeves, Function minimization by conjugate gradients, *Comput. J.* **7,** 149–154 (1964).
13. S. W. Provencher, A constrained regularization method for inverting data represented by linear algebraic or integral equations, *Comput. Phys. Commun.* **27,** 213–227 (1982).
14. P. Koehl, Linear prediction spectral analysis of NMR data, *Prog. NMR Spectrosc.* **34,** 257–299 (1999).
15. C. Airiau, F. Gaudard, A. S. Barros, and D. N. Rutledge, Complexation stoechimetry determined by application of chemometrics to time domain nuclear magnetic resonance signals, *Analusis* **26,** 70–741 (1998).
16. D. N. Rutledge, A Windows program for relaxation parameter estimation, *in* "Signal Treatment and Signal Analysis in NMR" (D. N. Rutledge, Ed.), pp. 191–217, Elsevier, Amsterdam (1996).
17. S. Karlin and L. S. Shapley, Geometry of moment spaces, *Mem. Am. Math. Soc.* **12,** 1–93 (1953).